ADVANCED MATERIALS

Supporting Information

for *Adv. Mater.*, DOI: 10.1002/adma.201903173

Enhanced Light Utilization in Semitransparent Organic Photovoltaics Using an Optical Outcoupling Architecture

Yongxi Li, Chengang Ji, Yue Qu, Xinjing Huang, Shaocong Hou, Chang-Zhi Li, Liang-Sheng Liao, L. Jay Guo, and Stephen R. Forrest**

Supplementary Information

Enhanced Light Utilization in Semi-Transparent Organic Photovoltaics Using an Optical Outcoupling Architecture

Yongxi Li[1, †], Chengang Ji[1, †], Yue Qu[1], Xinjing Huang[1], Shaocong Hou[1], Chang-Zhi Li[3], Liang-Sheng Liao[2], L. Jay Guo[1*] and Stephen R. Forrest[1*]

[1]*Departments of Electrical Engineering and Computer Science, University of Michigan, Ann Arbor, MI 48109, USA*

[2]*Institute of Functional Nano & Soft Materials (FUNSOM), Soochow University, Suzhou, Jiangsu 215123, P.R. China.*

[3]*Department of Polymer Science and Engineering, Zhejiang University, Hangzhou, 310027, P.R. China.*

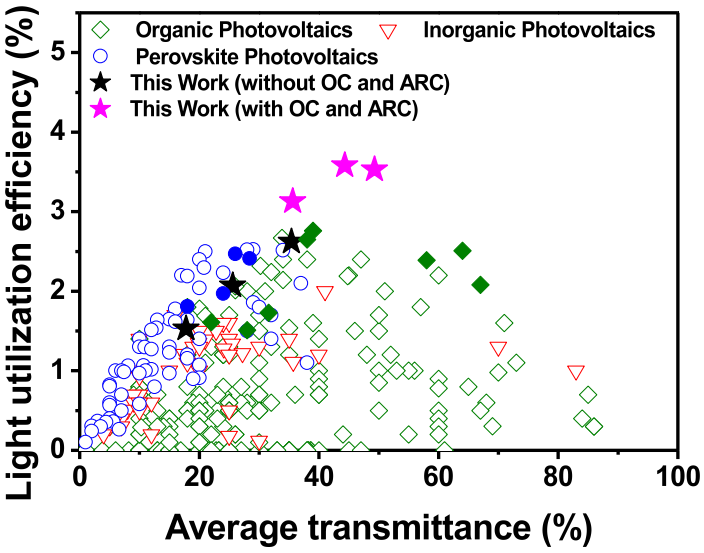

Supplementary Figure 1. Light utilization efficiency versus average transmittance for organic, inorganic and perovskite solar cells. (The solid data points represent recalculated average photopic transmittance, the empty points represent average visible transmittance from the literature. References are listed here only if the sum of the EQE, reflectivity and transmissivity are less than or equal to one.) References for the complete survey are provided in Supplementary Data 1[1].

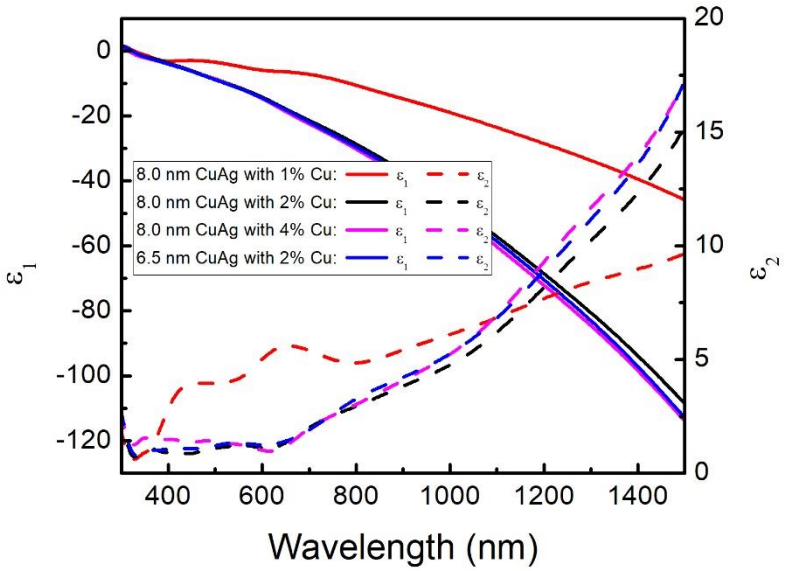

Supplementary Figure 2. Permittivity of thin Cu-Ag films deposited at various thicknesses and Cu concentrations.

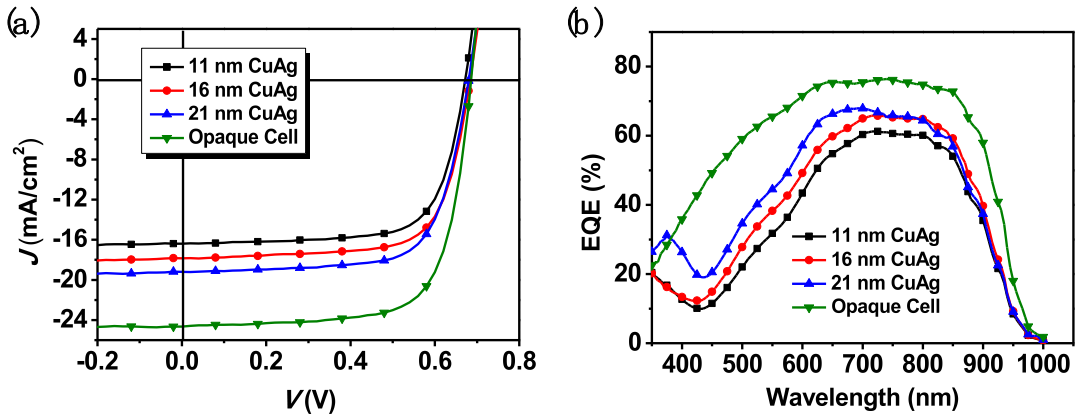

Supplementary Figure 3. a, Current-density-voltage characteristics. **b,** External quantum efficiency spectra of organic photovoltaics with different thickness of anode.

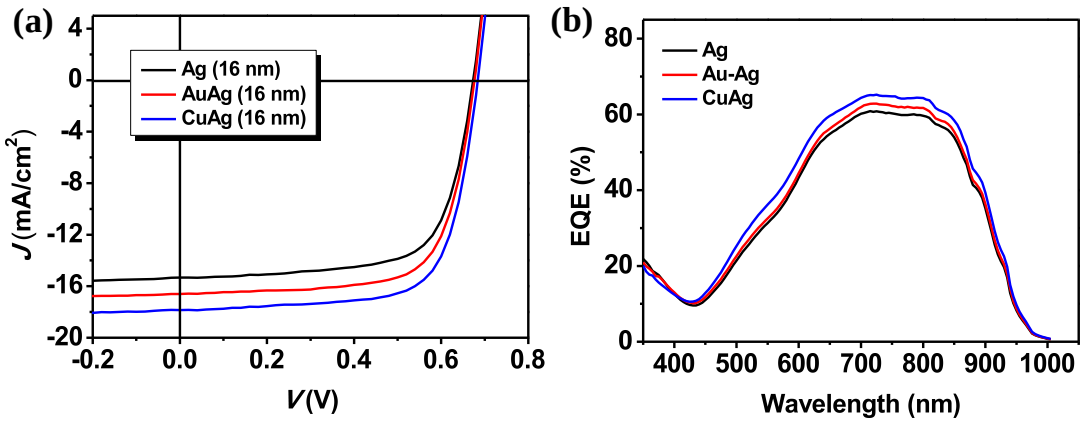

Supplementary Figure 4. a, Current-density-voltage characteristics. **b,** External quantum efficiency spectra of semi-transparent organic photovoltaics with different anodes.

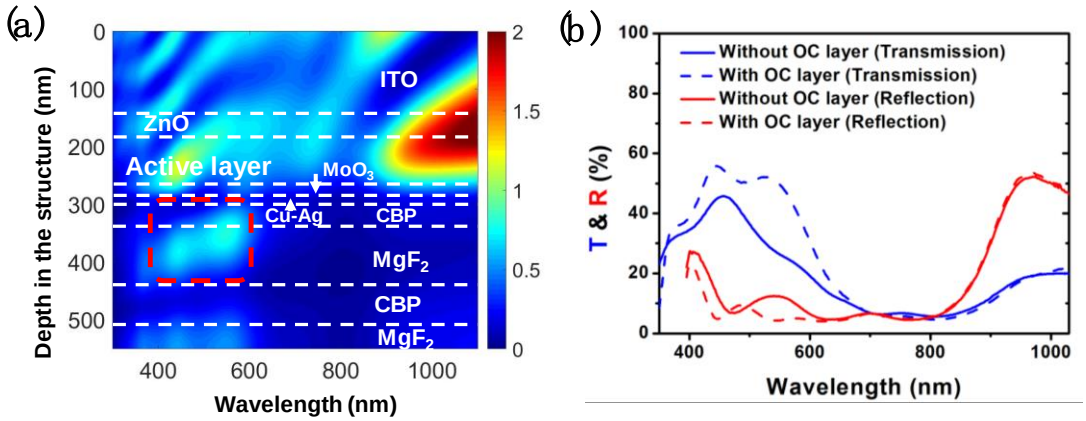

Supplementary Figure 5. a, Optical field distribution within the semitransparent solar cell based on the 16 nm Cu-Ag anode with the outcoupling layer. **b,** Measured reflection and transmission spectra of the semitransparent devices with and without outcoupling layer.

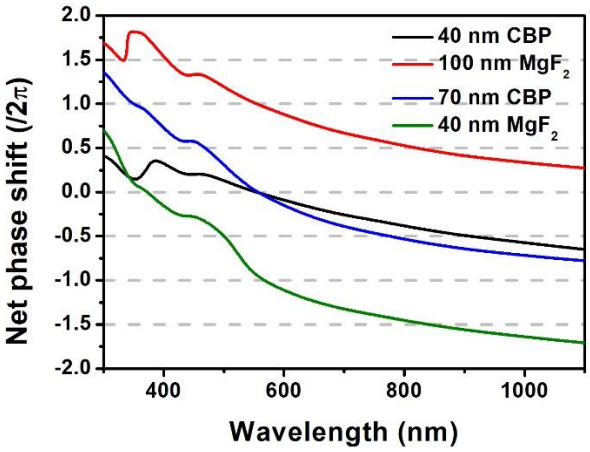

Supplementary Figure 6. The calculated net phase shift of each layer of the outcoupling structures as a function of the wavelength (16 nm Cu-Ag device).

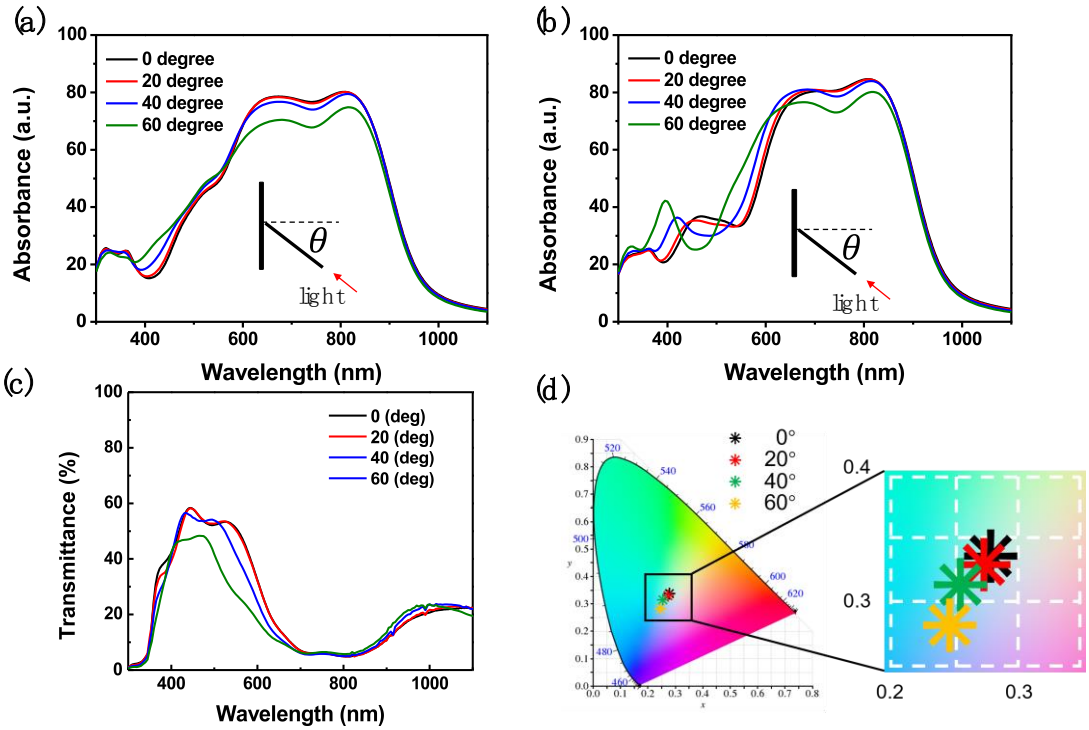

Supplementary Figure 7. a, Simulated absorption in the active layer of the semi-transparent devices (16 nm CuAg) without OC and ARC under different illumination angles. **b,** Simulated absorption in the active layer of the semi-transparent devices (16 nm CuAg) with OC and ARC under different illumination angles. **c,** Measured transmission spectra of the semi-transparent devices (16 nm CuAg) with OC and ARC under different illumination angles. **d,** CIE coordinates of the transmission spectra of devices with OC and ARC under different illumination angles using a AM1.5G solar simulated input spectrum.

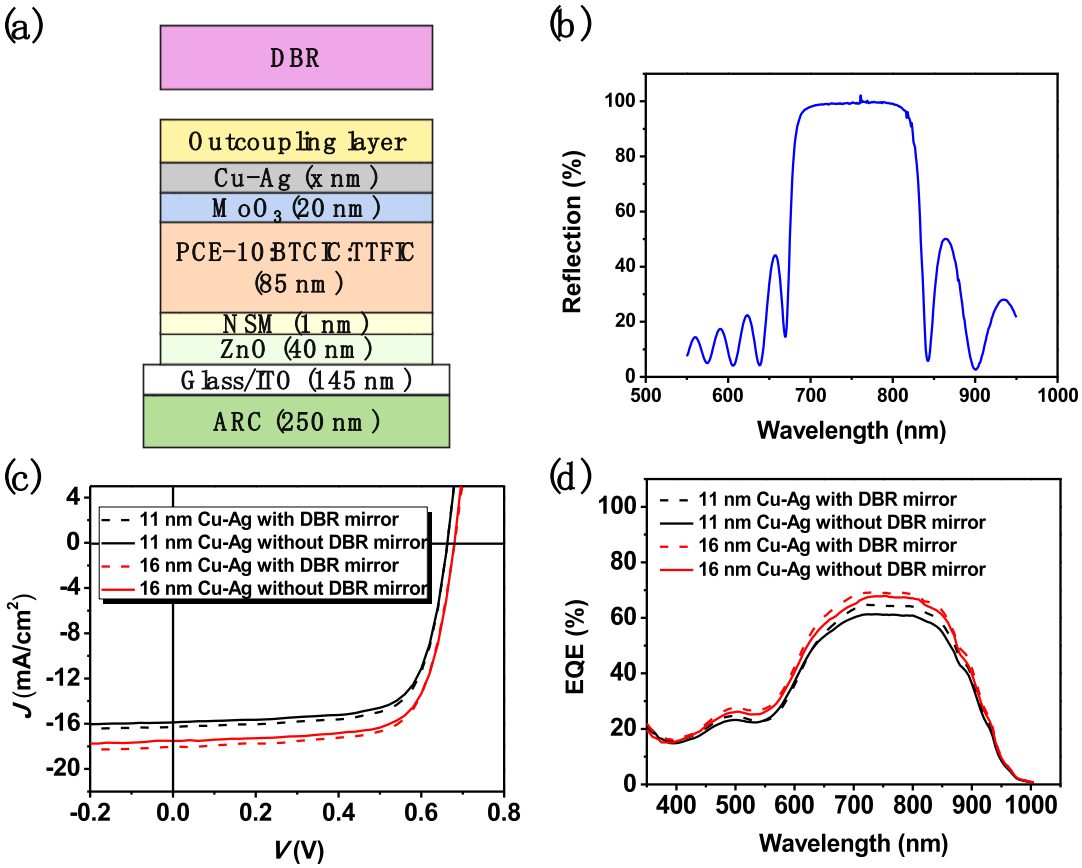

Supplementary Figure 8. a, Schematic of the semi-transparent device with a distributed Bragg reflector. **b,** Measured reflection spectrum of the distributed Bragg reflector. **c,** Current-density-voltage characteristics. **d,** External quantum efficiency spectra of semi-transparent solar cells with/without distributed Bragg reflector.

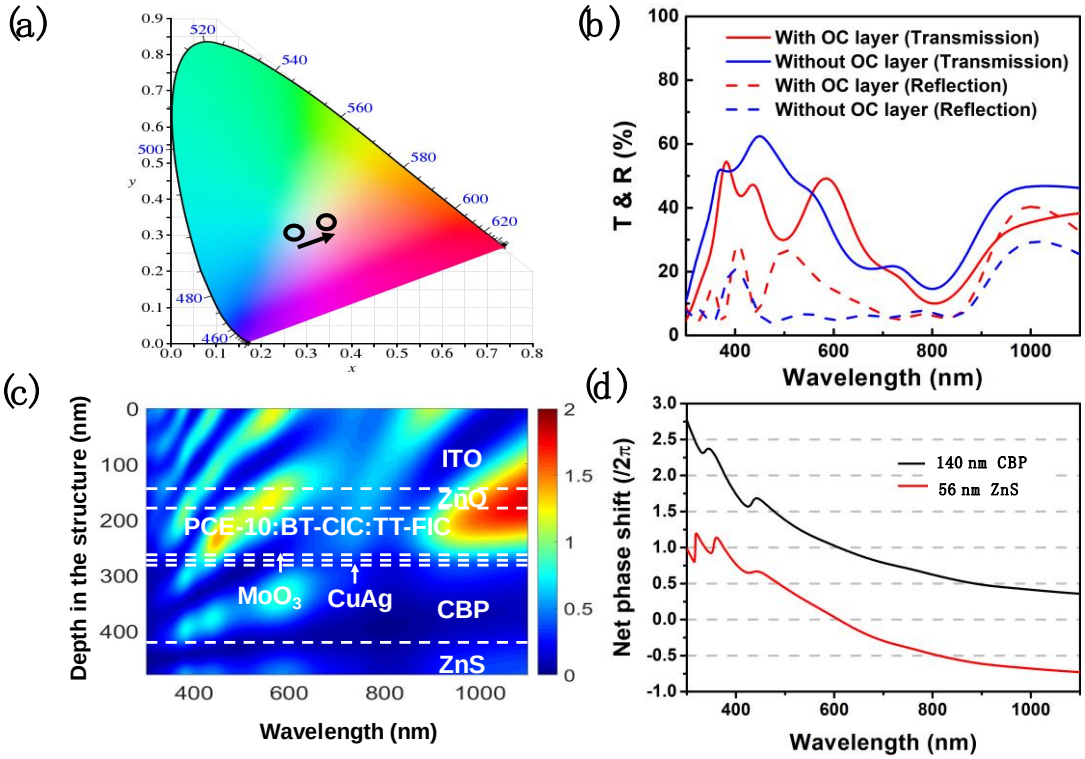

Supplementary Figure 9. a, Color coordinates on CIE 1931 chromaticity diagram of the transmission spectra of devices with and without outcoupling layer using a AM1.5G solar simulated input spectrum. **b,** Simulated reflection & transmission spectra of the semi-transparent devices with and without outcoupling layers. **c,** Optical field distribution of the neutral-colored semi-transparent solar cell. **d,** The calculated net phase shift of each layer of the outcoupling structures as a function of the wavelength.

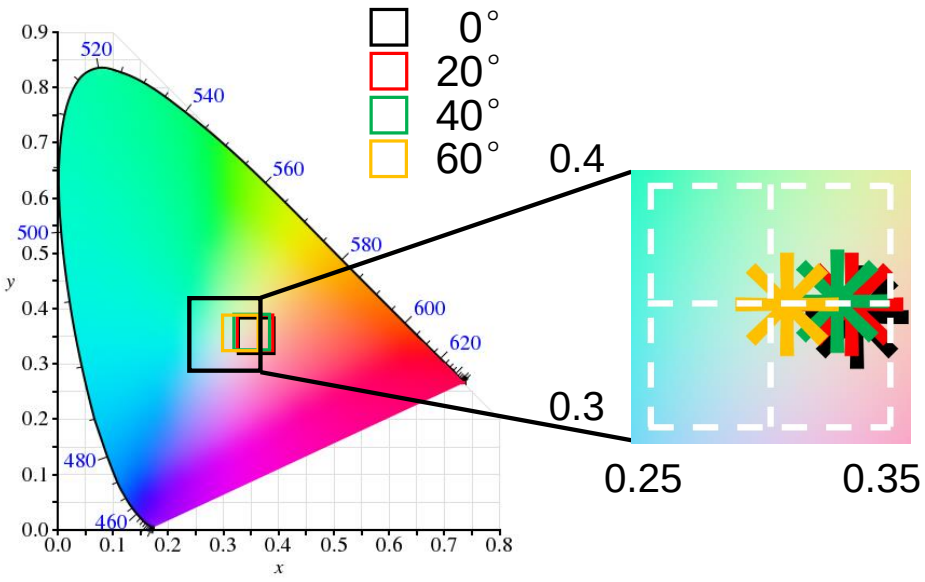

Supplementary Figure 10. CIE coordinates of the transmission spectra of the color-neutral ST-OPVs under different illumination angles using a AM1.5G solar simulated input spectrum.

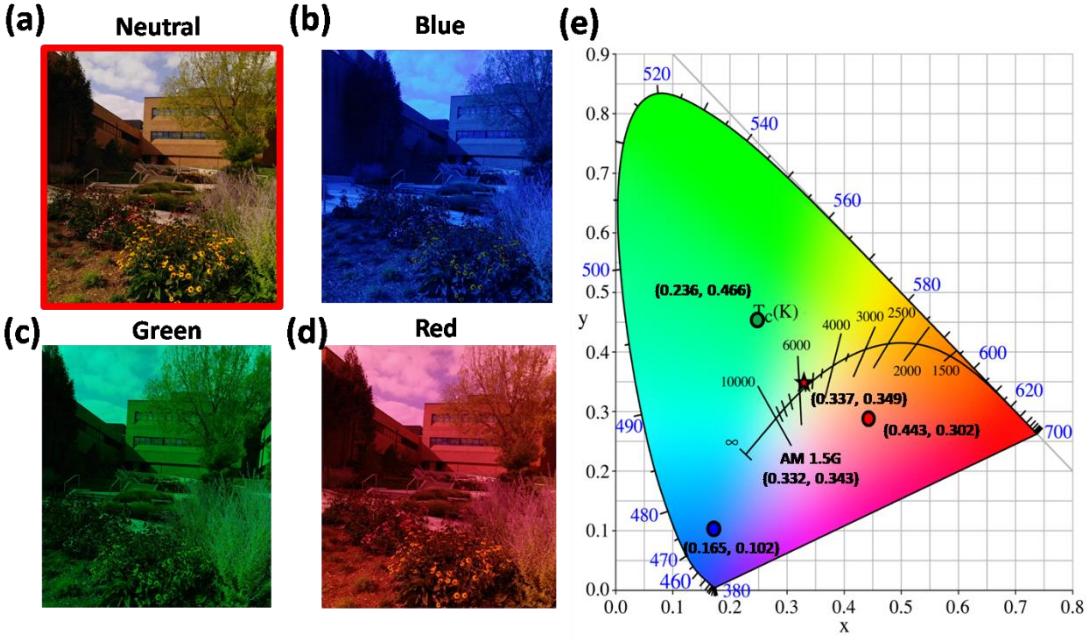

Supplementary Figure 11. a, Photograph of the outdoor image through the neutral color cell. **b,** blue cell. **c,** green cell. **d,** red cell. **e,** CIE coordinates of the transmission spectra of devices with different colors using a AM1.5G solar simulated input spectrum.

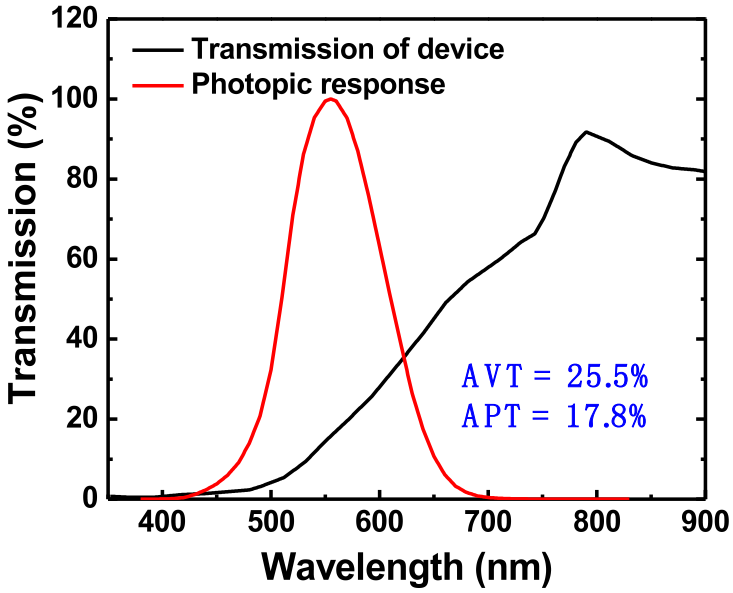

Supplementary Figure 12. Measured optical transmission of semitransparent cells and the photopic response. The transmission data are extracted from ref: *Chem. Mater.*, 2015, 27, 5122−5130.

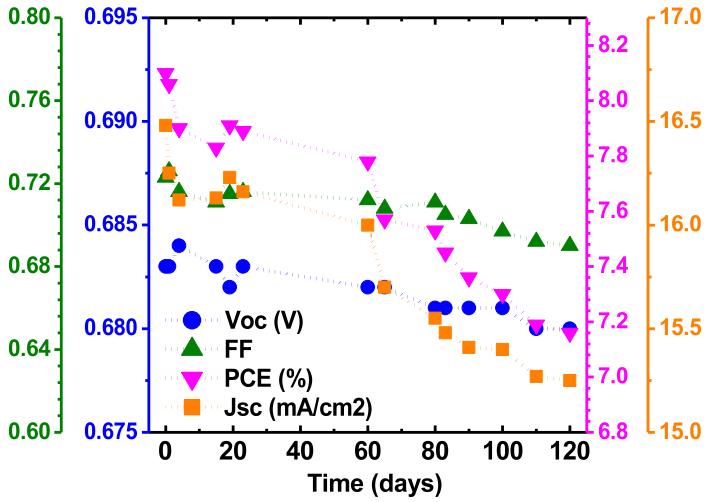

Supplementary Figure 13. Measured device parameters over time (16 nm Cu-Ag device with OC and ARC).

Table S1 | Operating characteristics of semi-transparent OPVs with different anodes under simulated AM 1.5G, 100 mW cm^{-2} illumination**.**

Device*	$J_{SC\ EQE}$ ***(mA/cm²)***	V_{OC} ***(V)***	***FF***	***PCE (%)***
Ag (16 nm)	15.1	0.68	0.69	7.1
Au-Ag (16 nm)	15.6	0.68	0.70	7.4
Cu-Ag (16 nm)	16.6	0.68	0.72	8.1

Table S2 | Operating characteristics of semi-transparent OPVs under simulated AM 1.5G, 100 mW cm^{-2} illumination**.**

Device*	$J_{SC\ EQE}$ [(a)] ***(mA/cm²)***	V_{OC} ***(V)***	***FF***	***PCE***[(b)] ***(%)***

11 nm Cu-Ag (with OC and ARC)	14.8 ± 0.3	0.67 ± 0.01	0.72 ± 0.01	7.2 ± 0.2
11 nm Cu-Ag (with DBR)	15.3 ± 0.3	0.67 ± 0.01	0.72 ± 0.01	7.4 ± 0.3
16 nm Cu-Ag (with OC and ARC)	16.2± 0.2	0.68 ± 0.01	0.72 ± 0.01	8.0 ± 0.2
16 nm Cu-Ag (with DBR)	16.8 ± 0.3	0.68 ± 0.01	0.71 ± 0.01	8.2 ± 0.3

[(a)]The J_{SC} values are calculated from the integral of the *EQE* spectrum.
[(b)]The *PCE* are calculated based on measurement of 8 devices.

Table S3| Operating characteristics of multi-colored semitransparent OPVs under simulated AM 1.5G, 100 mW cm^{-2} illumination**.**

Device	J_{SC} [(a)] (mA/cm^2)	V_{OC} (V)	*FF*	*PCE*[(b)] (%)	*AVT* (%)	*LUE* (%)
Blue	18.6	0.67	0.71	8.9	4.0	0.36
Green	18.1	0.68	0.71	8.7	17.0	1.48
Red	17.3	0.68	0.70	8.3	5.9	0.49
Neutral	13.2	0.65	0.67	5.8	44.3	2.57

(a) The J_{SC} values are calculated from the integral of the *EQE* spectrum.

(b) Calculated based on measurement of 8 devices.

Reference

[1] C. J. Traverse, R. Pandey, M. C. Barr, R. R. Lunt, *Nature Energy* **2017**, *2*, 849-860.